

COMPARISON OF LAND SURFACE TEMPERATURE MAPPING USING MODIS AND ASTER IMAGES IN SEMI-ARID AREA

M. Akhoondzadeh and M.R. Saradjian

Remote Sensing Division, Surveying and Geomatics Dept., Faculty of Engineering, University of Tehran, Tehran, Iran - makhonz@ut.ac.ir and sarajian@ut.ac.ir

Commission VIII, WG VIII/9

KEY WORDS: MODIS, ASTER, Land Surface Temperature (LST), Emissivity.

ABSTRACT:

This paper presents application of the Earth Observing System (EOS) Moderate Resolution Imaging Spectroradiometer (MODIS) thermal infrared bands for Land Surface Temperature (LST) retrieval. A brief summary of the Generalized split-window algorithm discuss and then LST map of Iran was calculated from Terra-MODIS 1km resolution images. For a given MODIS pixel, the split-window LST algorithm requires emissivities in band 31 and 32. These values are estimated by determining the MODIS/IGBP class and looking up the emissivity value in a table. After geometric correction of the image, LST of clear-sky pixels in MODIS scenes is retrieved from brightness temperatures in bands 31 and 32 in generalized split-window algorithm. The coefficient used in the split window algorithm are given by a LUT (Look-up table). Results compared using ASTER data acquired with same date and time. One study site selected: a semi-arid area located in south of Iran. The ASTER estimates were derived using the Temperature Emissivity Separation (TES) algorithm. The MODIS and ASTER temperature retrievals were in good agreement. It was shown that Classification-based emissivity is a good way for retrieval of temperature in Iran if Land-cover map would be refined with more information in the classification look-up scheme. In conclusion, the MODIS infrared images, because of their radiometric and spectral resolution and extensive swath width band can be useful for retrieval of LST map from Iran in different time periods for scientist studies.

1. INTRODUCTION

LST is a good indicator of the energy balance at the surface because it is one of the key parameters in the physics of land-surface processes. It combines the results of surface-atmosphere interactions and energy fluxes between the atmosphere and the ground.

LST is defined by the radiation emitted by the Land surface observed by MODIS at instant viewing angles. In order to understand the earth system better on the global scale, the earth observing system (EOS) will provide surface kinetic temperatures at specified accuracies of 0.3 K for oceans and 1 K for land. During the past decade, significant progress has been made in estimation of land surface emissivity and temperature from airborne thermal infrared data. Kahle et al, developed a technique to estimate the surface temperature based on an assumed constant emissivity in one channel and previously determined atmospheric parameters. This temperature was then used to estimate the emissivity in other channels. Other techniques, such as thermal log residuals and alpha residuals, have been recently developed to extract emissivity information from multispectral thermal infrared data. A variety of split-window methods have been developed to retrieve sea-surface temperature and land-surface temperature from NOAA AVHRR data. A major problem in using split-window LST methods is that we need to know the surface emissivities in the bands better than 0.01.

A look-up table for classification-based land surface emissivity in the thermal infrared (TIR) is useful for various studies involving energy balance and global circulation models, and surface temperature measurement from space. Our motivation is to develop an emissivity knowledge base to be used in

conjunction with a split-window algorithm for land surface temperature (LST). Also sensor zenith angles used in split window algorithm for increase of accuracy. The split-window method corrects for atmosphere effects based on the differential absorption in adjacent infrared bands.

2. METHOD

In classification-based method a pixel is classified as one of fourteen emissivity classes based on the conventional land cover classification and dynamic and seasonal factors, such as snow cover and vegetation index. In this study we used land cover map from Iran that has been produced by Iran space agency (fig. 1).

This emissivity models, provide a range of values for each emissivity class by combining various spectral component measurements with structural factors (Wan and Snyder, 1998). emissivity statistics are reported for the EOS/MODIS channels 31 and 32, which are the channels that will be used in the LST split-window algorithm (Table 1,2).

A look-up table for classification-based global land surface emissivity in the thermal infrared (TIR) is useful for various studies involving energy balance and circulation models, and surface temperature measurement from space. We develop an emissivity knowledge base to be used in conjunction with a split-window algorithm for land surface temperature for moderate resolution imaging spectrometer (MODIS).

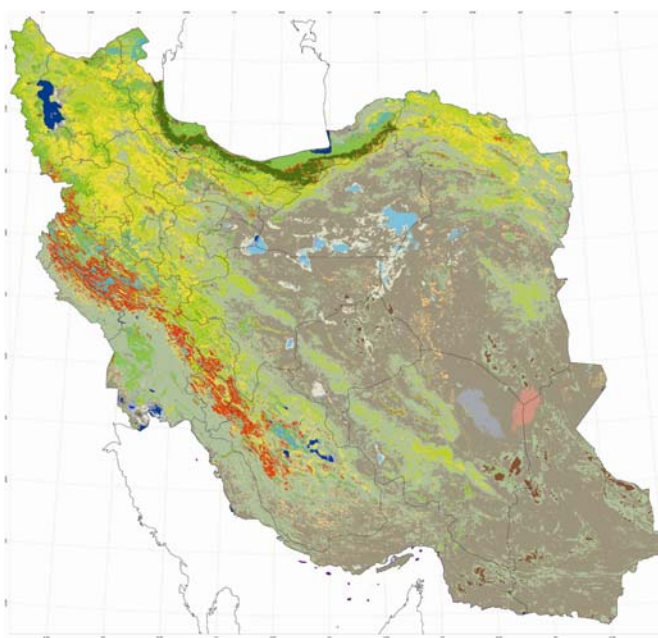


Figure 1. Iran land cover map

Emissivity class	Angle			
	10°	40°	65°	
Gr. Ndle. Forest	0.989	0.002	0.989	0.002
Sn. Ndle. Forest	0.986	0.003	0.986	0.003
Gr. Bdfl. Forest	0.987	0.003	0.987	0.003
*Sn. Bdfl. Forest	0.968	0.016	0.967	0.017
Gr. Woody Savanna	0.988	0.004	0.988	0.004
Sn. Woody Savanna	0.975	0.010	0.976	0.010
Gr. Grass Savanna	0.987	0.003	0.987	0.003
Sn. Grass Savanna	0.973	0.013	0.973	0.013
*Gr. Sparse Shrubs	0.972	0.006	0.973	0.007
*Sn. Sparse Shrubs	0.970	0.005	0.971	0.005
*Water	0.991	0.001	0.992	0.003
Org. Bare Soil	0.977	0.010	0.977	0.010
*Arid Bare Soil	0.966	0.017	0.965	0.017
Snow, Ice	0.988	0.006	0.988	0.006

= Classes with angular variation in band 31 that is 0.002° or above.

Table 1. Modeled angular effects band 31 for the fourteen emissivity classes.

Emissivity class	Angle			
	10°	40°	65°	
Gr. Ndle. Forest	0.991	0.003	0.991	0.003
Sn. Ndle. Forest	0.988	0.004	0.987	0.004
Gr. Bdfl. Forest	0.990	0.004	0.990	0.004
*Sn. Bdfl. Forest	0.971	0.009	0.970	0.010
Gr. Woody Savanna	0.991	0.003	0.991	0.004
Sn. Woody Savanna	0.978	0.009	0.978	0.009
Gr. Grass Savanna	0.991	0.003	0.991	0.003
Sn. Grass Savanna	0.975	0.011	0.975	0.011
*Gr. Sparse Shrubs	0.976	0.014	0.977	0.014
Sn. Sparse Shrubs	0.975	0.014	0.975	0.014
*Water	0.986	0.002	0.988	0.006
Org. Bare Soil	0.982	0.007	0.982	0.007
Arid Bare Soil	0.972	0.016	0.972	0.016
*Snow, Ice	0.977	0.013	0.979	0.012

Classes with angular variation in band 32 of 0.002° or above.

Table 2. Modeled angular effects band 32 for the fourteen emissivity classes.

MODIS is an EOS instrument that will serve as the keystone for global studies of atmosphere, land and ocean processes. It scans $\pm 55^\circ$ from nadir in 36 bands, with bands 1-19 and band 26 in the visible and near infrared range, and the remaining bands in the thermal infrared from 3-15 μm . The

36-band MODIS satellite scanner has 1 km^2 pixels at nadir for the thermal infrared bands that will be used for LST. The proposed algorithm employs the radiance and emissivity in band 31 and band 32. With 15 emissive bands, the Moderate Resolution Imaging Spectroradiometer (MODIS) on-board the EOS-TERRA platform offers new perspective in earth observation in the infrared spectrum (3-15 μm). Because chemical components of the atmosphere have various absorption bands, only seven MODIS emissive bands are useful for land surface remote sensing. MODIS has four bands (20, 21, 22, 23) in the 3-5 μm atmospheric window. Surface properties in the infrared are specified either in terms of emissivity or reflectance, the emissivity being related to the directional hemispheric reflectance by Kirchhoff's law.

The emissivity estimation is accomplished by the use of linear bidirectional reflectance distribution function (BRDF) models, which have spectral coefficients derived from laboratory measurements of material samples and have structural parameters derived from approximate descriptions of the cover type (Snyder and Wan 1998). The emissivity of a surface is a function of many factors, including water content, chemical composition, structure and roughness. The identification of surface moisture for improved emissivity estimates is under investigation. We will need to apply more information in the classification look-up scheme to refine the estimates.

For a given MODIS pixel, the split-window LST algorithm requires emissivities in bands 31 and 32.

$$T_s = (A_1 + A_2 \frac{1-\varepsilon}{\varepsilon} + A_3 \frac{\Delta\varepsilon}{\varepsilon^2}) \frac{T_{31} + T_{32}}{2} + (B_1 + B_2 \frac{1-\varepsilon}{\varepsilon} + B_3 \frac{\Delta\varepsilon}{\varepsilon^2}) \frac{T_{31} - T_{32}}{2} + C \quad (1)$$

where $\Delta\varepsilon = (\varepsilon_{31} - \varepsilon_{32})$ and $\varepsilon = 0.5(\varepsilon_{31} + \varepsilon_{32})$ are the difference and mean of surface emissivities in MODIS band 31 and 32. T_{31} and T_{32} are the brightness temperatures in these two split-window bands.

The coefficients $A_1, A_2, A_3, B_1, B_2, B_3, C$ are given by interpolation on asset of multi-dimensional look-up tables (LUT).

The Lut were obtained by linear regression the MODIS simulation data from radiative transfer calculations over wide range of surface and atmospheric conditions.

These values are estimated by determining the MODIS/IGBP class and dynamic state of that pixel and looking up the emissivity value in a table. The emissivity for all cover types in bands 31 and 32 will eventually need to be estimated to an accuracy of better than 0.005 units and these estimates will

need to be unbiased to support long-term global environmental studies.

it seems possible to have such knowledge of the emissivities for certain types of land covers, such as lake surfaces, snow/ice, dense evergreen canopies, and some soils. For land covers with variable emissivities, especially in semi-arid and arid areas, it is almost impossible to estimate two band-averaged emissivities to such accuracy.

3. SATELLITE DATA PROCESSING

Several data-processing steps are necessary before implementing the LST split-window algorithm. The digital signal in each channel is converted into an apparent radiance value for the sensor. Planetary reflectance or brightness temperatures are then calculated, including the effects of illumination and view angle. Geometric distortion, which depends on the relative position of the earth and the satellite, the satellite's attitude, the rotation of the earth, the satellite's velocity, the scan velocity, etc., is then corrected. This correction uses a set of ground control points and is applied for each image using polynomial equations in a nearest-neighbour re-sampling method in the ERDAS image processing software. Cloud detection and cloud masking are important, because a major sources of error in the retrieval of LST from thermal infrared satellite data is cloud contamination. Therefore, the detection and elimination of totally or partly cloudy pixels is necessary before further data processing. Most cloud-detection algorithms use successive tests that include different channels in the visible and infrared parts of the spectrum. MODIS image from iran in 30 Jan 2004 selected for processing and was corrected for geometric correction (Fig. 2).

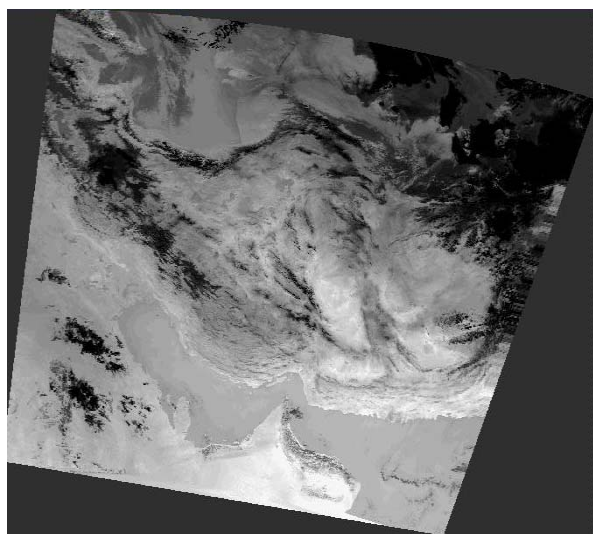


Figure 2. MODIS image from Iran (2004/01/30) after Geometric correction.

It is also important to consider carefully the effect of the atmosphere on the image of the remotely sensed surface. Brightness temperatures were extracted from measured radiance using inverse Plank's law (2).

$$T = \frac{\left(\frac{hc}{k}\right)}{\lambda * \ln\left(\frac{2hc^2}{L\lambda^5} + 1\right)} \quad (2)$$

Where k is stefan boltzmann constant, h is plank constant, L is radiance and T is brightness temperature.

With replacement of brightness temperature and emissivities (band 31 , 32) in split-window algorithm Iran LST map was generated (Fig. 3).

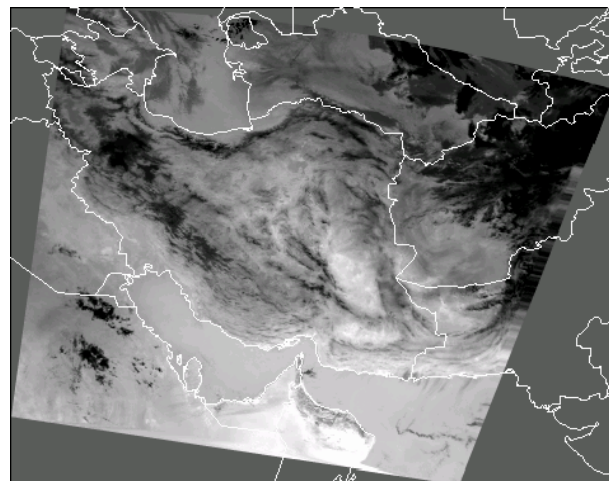


Figure 3. Iran LST map in date 2004/01/30

4. ANALYSIS AND COMPARISON

Because ground-based measurement of LST was not available for the present study, we employed the LST map that was generated from ASTER data in same date by TES (Temperature Emissivity Separation) (Fig. 4). Both ASTER and MODIS are on EOS-TERRA, a sun-synchronous platform with a 10:30 am descending equator crossing. The ASTER TIR sensor is a five-band with a 90 m spatial resolution and a 63 km swath. The TES algorithm combines interesting features of three approaches: Normalized Emissivity method, Ratio Algorithm and Maximum Minimum Difference.

We compare two LST maps (MODIS and ASTER) with 92 control points. Results of this comparison showed (Fig. 5 , 6) these products are in good agreement and RMS error was $1.487^\circ k$.

5. CONCLUSION

The scope of this study was to compare estimates of land surface temperature derived from measurements collected using the MODIS and ASTER sensors. The MODIS and ASTER emissivities estimates were retrieved using the classification-based algorithm and the TES algorithm respectively. Such investigations were of interest since the algorithms relied on different assumptions according to the temporal, spectral and directional information provided by each sensor. The comparison between MODIS and ASTER retrievals was possible since ASTER and MODIS are on board the same platform, which eliminated temporal problems due to the non

stable nature of kinetic temperature. Results of this comparison was in good agreement and can be better if atmospheric corrections and calculation of emissivity will be done with high accuracy.

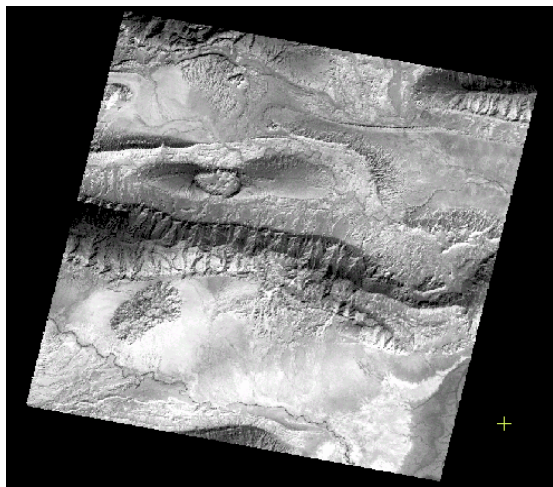


Figure 4. LST map generated by ASTER data

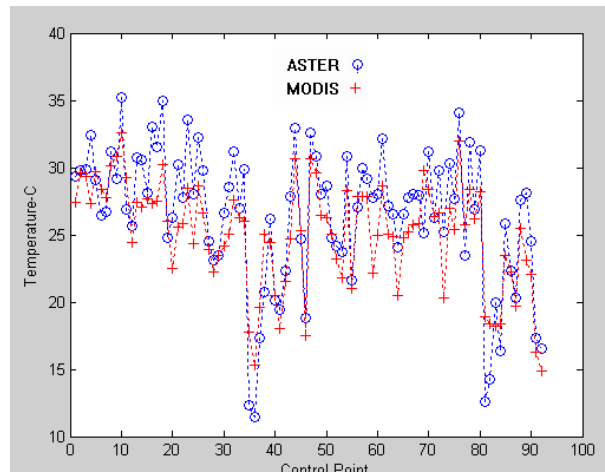


Figure 5. LST values for 92 control points in MODIS and ASTER

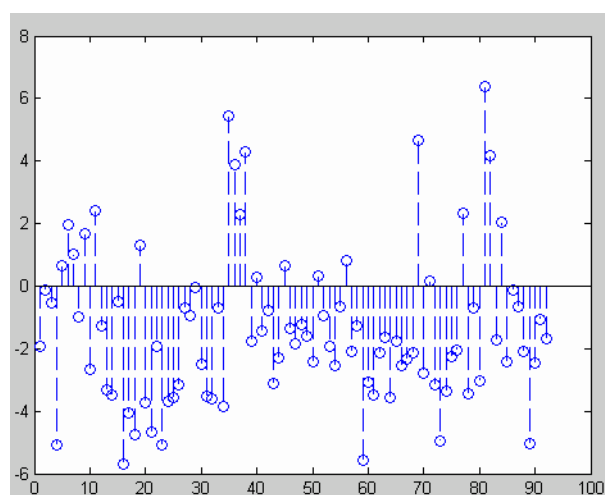


Figure 6. Differences of LST values for 92 control points in MODIS and ASTER

REFERENCES

- BECKER, F., and LI, Z. L., 1990. Temperature Independent Spectral Indices in thermal infrared bands. *Remote Sensing of Environment*, 32, 17-33.
- BECKER, F., and LI, Z. L., 1995. Surface Temperature and emissivity at various scales: definition, measurement and related problems. *Remote Sensing of Environment*, 12, 225-253.
- PETITCOLIN, F., and VERMOTE, E., 2002. Land surface reflectance, emissivity and temperature from MODIS middle and thermal infrared data. *Remote Sensing of Environment*, 83, 112-134.
- PRICE, J. C., 1983. Estimating surface temperature from satellite thermal infrared data. *Remote Sensing of Environment*, 13, 353-361.
- SALISBURY, J. W., AND D'ARIA, D. M., 1992. Emissivity of terrestrial materials in the 8-14 μm atmospheric window. *Remote Sensing of Environment*, 42, 83-106.
- SALISBURY, J. W., AND D'ARIA, D. M., 1994. Emissivity of terrestrial materials in the 3-5 μm atmospheric window. *Remote Sensing of Environment*, 42, 345-361.
- SALISBURY, J. W., AND D'ARIA, D. M., and WALD, A., 1994. Measurement of thermal infrared spectral reflectance of frost, snow, and ice. *Journal of Geophysics Research*, 99, 24,235-24,240.
- SNYDER, W.C., and WAN, Z., ZHANG, Y., and FENG, Y., 1997. Thermal infrared (3-14 μm) bidirectional reflectance measurement of sands and soils. *Remote Sensing of Environment*, 60, 101-109.
- SNYDER, W.C., and WAN, Z., ZHANG, Y., and FENG, Y., 1998. Classification-based emissivity for land surface temperature measurement from space. *International Journal of Remote Sensing*, 19(14), 2753-2774.
- WAN, Z., and DOZIER, J., 1996. A generalized split-window algorithm for retrieving land-surface temperature from space. *IEEE Transactions on Geoscience and Remote Sensing*, 34, 892-905.
- WAN, Z., and LI, Z., 1997. A physics-based algorithm for retrieving land-surface emissivities and temperature from EOS/MODIS data. *IEEE Transactions on Geoscience and Remote Sensing*, 35, 980-996.
- WAN, Z., ZHANG, Y., ZHANG, Q., and LI, Z., 2002. Validation of the land-surface temperature products retrieved from Terra Moderate Resolution Imaging Spectroradiometer data. *Remote Sensing of Environment*, 83, 163-180.
- WAN, Z., ZHANG, Y., ZHANG, Q., and LI, Z., 2004. Quality assessment and validation of the MODIS global land surface temperature. *International Journal of Remote Sensing*, 25(1), 261-274.